RSC Advances

REVIEW

View Article Online
View Journal | View Issue

Cite this: *RSC Adv.*, 2016, **6**, 6788

Platinum nanocatalysts on metal oxide based supports for low temperature fuel cell applications

N. R. Elezovic,*[a] V. R. Radmilovic[b] and N. V. Krstajic[b]

Received 26th October 2015
Accepted 28th December 2015

DOI: 10.1039/c5ra22403a

www.rsc.org/advances

In this manuscript a survey of the contemporary research related to platinum nanocatalysts on metal oxide based supports for low temperature fuel cell applications is presented. Different carbon based supports, used as state of the art materials, are listed and discussed, as well. Although carbon based materials possess many desirable properties, such as high surface area, high conductivity and relatively low cost and easy synthesis, the large scale commercialization is limited by instability under accelerated stability testing, simulating real fuel cell operating conditions. To overcome these disadvantages of carbon supports, different metal oxide based ones have been studied and promising results are referenced. The most often used oxide based supports for low temperature fuel cell applications are presented in this review. Suitable discussion and future research related remarks are given, as well.

1. Introduction

Polymer electrolyte membrane fuel cells (PEMFCs) are promising candidates for an environmentally friendly and efficient energy conversion, with many prospective practical applications in portable, stationary and transport devices. In spite of researchers' efforts during last few decades, many challenges in this field still remain unresolved. The main issues are still insufficient catalysts activity and stability, to decrease high costs, and relatively low life time of PEMFCs. Therefore, activity, stability and durability are major problems in this field and key points limiting the commercialization.[1] It is well known that the whole cell performance is significantly influenced by the oxygen reduction reaction, owing to its slow kinetics and much higher overpotential, if compared to fast anodic hydrogen oxidation. Namely, the thermodynamic reversible potential for oxygen reaction on Pt is 1.23 V. Reversible hydrogen electrode, while the real open circuit potential value established *vs.* the same reference electrode is about 0.3 V lower. This large potential loss was attributed to the fact that the surface of Pt was covered with oxygen containing species from water (*e.g.* OH), or other adsorbed anions. Thus, the main source of energy losses in fuel cells is the oxygen reduction reaction.[2] Platinum nanocatalysts on high surface area carbon based supports exhibit the best catalytic activity and stability for reactions taking place in fuel cell: oxygen reduction and hydrogen oxidation.[2–6]

Pt nanoparticles homogeneously distributed over carbon support (commercially named Vulcan and Ketjen black) are state of the art catalyst materials for both anode and cathode reactions. However, high cost and scarcity of platinum are the main problems to be solved before commercialization of these clean energy providers. Many efforts have been made to achieve sufficient low Pt loading (mg_{Pt} cm^{-2}) to gain satisfactory power density: 0.9–1.2 g_{Pt} kW^{-1}, for stationary, uninterrupted power supply, while less than 0.4 g_{Pt} kW^{-1} for large scale commercialization in automotive applications is required.[7] Limited durability caused by degradation of the carbon support, usually used in commercially available Pt catalysts, increases total fuel cell costs and reduces its life time.[8] One of the key requirements for this class of fuel cells application is that the fuel cell must be tolerant of frequent start–stop cycling. During startup and shutdown procedure high potential difference is created, causing carbon corrosion and oxygen evolution on the air cathode. This mechanism has been called "reverse-current decay mechanism".[9] Namely, carbon corrosion could cause permanent carbon loss, loss of the catalytic activity, even the whole catalyst degradation. Platinum further accelerates the carbon corrosion rate, leading to agglomeration of the catalyst particles and severe degradation of fuel cell cathode. The key contemporary research activities in this field are: (a) development and characterization of new interactive metal oxide based supports with improved durability for fuel cells application (molybdenum, titanium oxide, tin oxide based supports); (b) development and characterization of new Pt nanocatalysts on above mentioned supports, to improve activity, to achieve commercially acceptable power density, mentioned above.

[a]*Institute for Multidisciplinary Research, University of Belgrade, Kneza Viseslava 1, Belgrade, Serbia. E-mail: nelezovic@tmf.bg.ac.rs*

[b]*Faculty of Technology and Metallurgy University of Belgrade, Karnegijeva 4, Belgrade, Serbia*

2. Carbon supported Pt nanocatalysts – state of the art materials for low temperature fuel cells application

The most used supports for low temperature fuel cells catalysts are carbon based. Namely, different carbon based materials were applied as platinum nanoparticles support owing to their properties: high surface area, relatively good chemical stability and well known synthesis procedures. A numerous papers were published, describing kinetics of oxygen reduction and hydrogen oxidation reactions at carbon supported platinum nanocatalysts in both acid and alkaline solutions.[10–15] Pt nanoparticles dispersed on different types of high surface area and electrical conducting carbon based supports were studied: carbon powder, carbon nanotubes, fullerenes are shown to have high electrocatalyst activity. The Pt loading has been reduced significantly with improved Pt utilization.[10–15] It was also clearly indicated that carbon support contributes itself to the kinetics of oxygen reduction in alkaline electrolyte, while in acid its contribution could be neglected.[16] The effect of Pt particle size on the oxygen reduction electrocatalysis in both electrolytes was correlated with the predominant facets of the platinum crystallites.[16] Tamizhmani *et al.*[17] and Markovic *et al.*[18] emphasized the crucial role of anion adsorption affects that could be cause of discrepancy and disagreement on the results and conclusions, related to specific and mass activities of the carbon supported catalysts in different electrolytes. The effect of the platinum particle size on the catalytic activity of Pt/Vulcan catalysts for oxygen reduction reaction has been studied and the loss of catalytic activity with the particle size decrease was demonstrated.[19] Namely, the specific activity was three times lower for very small particles. The activity decrease seems to be related to a strong adsorption of oxygenated species on very small particles: on cyclic voltammograms recorded for various platinum particle sizes a shift of desorption peak of the oxygenated species was observed.[19] Paulus *et al.* developed thin-film rotating disk electrode method and its application in a rotating ring disk configuration (RRDE) to the investigation of the oxygen reduction reaction on a supported catalyst powder (Pt:Vulcan XC 72 carbon).[20] RRDE measurements allowed, for the first time, the direct determination of the fraction of peroxide production during oxygen reduction on carbon supported Pt catalysts.[20] The comparison of the catalyst activity in H_2SO_4 and $HClO_4$ solution revealed a significant effect of (bi) sulfate adsorption on the ORR activity. Namely, the mass-specific current densities in the non-specifically adsorbing electrolyte were significantly higher than in 0.5 M H_2SO_4 while the fraction of H_2O_2 formation was almost the same.[20]

As the Nafion polymer is used for polymer electrolyte fuel cells it implies demand to explore its influence on catalytic activity of the Pt nanocatalysts. A. Ayad *et al.* investigated the kinetics of the reduction of oxygen on platinum covered by a Nafion® film in sulfuric in order to determine to what extent the polymer electrolyte modifies this reaction.[21] The cyclic voltammogram obtained for platinum covered with a Nafion® film was similar to that for bare platinum. Namely, the essential difference was that the hydrogen adsorption/desorption peaks were weaker, which indicates that some active sites had been filled in by the Nafion®. The proportion of active sites blocked by Nafion® was estimated from 15% to 20%.[22] It was also shown that the presence of Nafion® did not modify the kinetic parameters of oxygen reduction. The influence of Nafion was investigated by Z. Liu *et al.*[23] Nafion stabilized Pt nanoparticles showed considerable activity for the oxygen reduction but very low activity for the methanol oxidation reaction, in comparison to a conventional unsupported Pt black electrocatalyst. This indicates that Nafion stabilizer has strong inhibiting effect on the methanol oxidation reaction. Thus, Nafion-stabilized Pt nanoparticles are potential methanol tolerant electrocatalysts for the O_2 reduction reaction in DMFCs.[23] Curnick *et al.*[24] reported a facile method for the synthesis of stable and well-dispersed Nafion stabilized colloidal Pt nanoparticles with sizes in the range 3–10 nm. The activity for oxygen reduction was comparable with the commercial E-Tek catalyst. Combined with the near-100% utilisation measured at lower overall ionomer content for the Nafion1-Pt/C A catalysts, this implies that Pt nanoparticles synthesised with Nafion1 as a stabilizer can be 'tuned' to have simultaneous access to the reactant gas, the electron conducting carbon support and the proton conducting polymer electrolyte in the catalyst layer.[24]

Mayrhofer *et al.*[25] scrutinized the thin-film rotating disc electrode (TF-RDE) method for testing the catalytic activity of high surface area catalysts, especially oxygen reduction reaction at carbon supported platinum nanocatalysts. It was referred that carbon supported high surface area Pt catalysts exhibited better activity in comparison to polycrystalline platinum. The most important conditions that have to be fulfilled for accurate estimation of high surface area catalysts activity were emphasized:[25] (a) for a meaningful comparison of catalysts, normalized activities have to be determined rather than simply comparing polarization curves. The normalization can be based on the Pt loading (mass activity) or surface area (specific activity); (b) for the determination of the mass activity the complete utilization of the catalyst is mandatory. That is, the ECA has to be linear dependent on the loading. For the determination of the specific activity the active surface area has to be evaluated by applying a proper method that also considers the capacity of the support; (c) the diffusion limited current id of the ORR has to be within 10% of the theoretical value; (d) the current at the potential of interest (for the ORR usually in the region of 0.85–0.9 VRHE) has to be within 10% and 80% of the diffusion limited current, ideally below the half wave potential. Mayrhofer *et al.*[25] also suggested importance of determination optimal Pt loading for the rotating disc measurements. Namely, due to low Pt loading RDE could not be completely and homogenously covered. On the contrary, too high Pt loading implies that mass transport characteristics of the RDE are no longer satisfied. This is illustrated in Fig. 1.

Yoshii *et al.*[26] establishment of a facile Pt nanoparticle–SWCNT composite fabrication method that never requires a laborious pretreatment of SWCNTs or any chemical reagent was achieved by using Pt sputtered room temperature ionic liquid (RTIL). They found that RTIL can work as nanoglue for

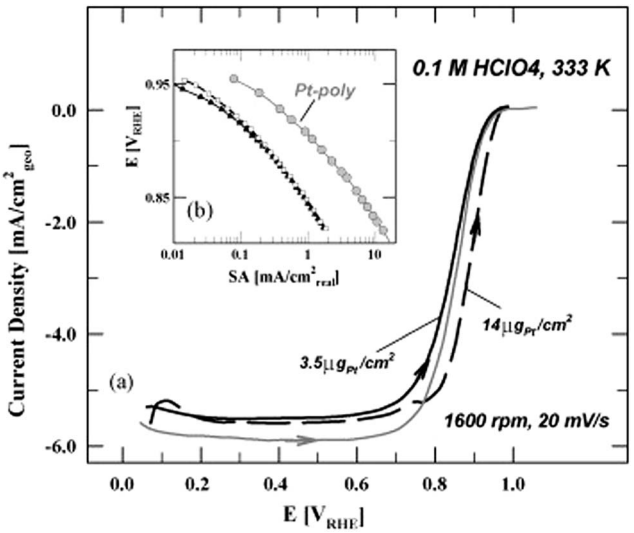

Fig. 1 ORR-polarization (a) curves for Pt-poly and the 1 nm catalyst with two different Pt loadings in 0.1 M $HClO_4$. The temperature is 333 K, sweep rate 20 mV s^{-1} and the rotation rate 1600 rpm. Only the anodic sweep is displayed for all samples. The estimated specific activities are presented in a Tafel-plot (b). Reprinted from the Electrochimica Acta in ref. 25, with permission of Elsevier.

sticking Pt nanoparticles against SWCNTs. This approach enabled variations in the amount of Pt nanoparticle and Pt particle size supported on the Pt–SWCNT composite by changing the sputtering time and/or RTIL species in the Pt sputtering process Pt–SWCNT composite expressed a promising catalytic activity for electrochemical ORR.[26] Speder *et al.*[27] prepared Pt nanoparticles supported on high surface area carbon by a colloidal method. The electrocatalysts synthesized by this method have well-separated, size-controlled nanoparticles with tunable interparticle distance, and thus enable the examination of the particle proximity effect on the oxygen reduction reaction (ORR). The particle proximity effect implies that the activity of fuel cell catalysts depends on the distance between the catalyst particles and it was for the first time demonstrated for high surface area catalysts. Based on rotating disk electrode (RDE) experiments, it was shown that the kinetic current density of ORR depends on the distance between the neighboring nanoparticles, *i.e.* the ORR activity increases with decreasing interparticle distance.[27] Singh *et al.*[28] demonstrated a highly efficient approach for the effective dispersion and excellent decoration of Pt nanoparticles on both sides of carbon nanofibers, targeted to improve the Pt utilisation for methanol electrooxidation. This method has enabled the achievement of fine dispersion fine and excellent decoration of carbon nanofibers. The possibility of both side deposition improves the effective surface area as well as particle dispersion, increasing the efficiency and utilization of both nanofibers and Pt. This nanocatalysts could be very promising solutions to Pt dissolution/stability issues, indicating the antipoisoning strength and capability to be used in fuel cell applications.[28] An ensemble of reduced functionalized graphene oxide, f-GO sheets and multiwalled carbon nanotubes (MWNTs), so called "few-layer graphene-MWNT sandwiches" (GCSs), were synthesized by a catalysis-assisted chemical vapor deposition (CCVD) method and explored as the electrocatalyst support material for oxygen reduction reaction (ORR) in a proton exchange membrane fuel cell (PEMFC).[29] The Pt nanocatalyst deposited onto this support gave a maximum PEMFC performance of 495 mW cm^{-2} at 60 °C temperature. The improvement in the ORR activity was ascribed to the uniform dispersion of Pt nanoparticles with an optimal particle size (3.5 nm) over a well-organized conducting catalyst support.[29] Pt-based nanoparticles on non-covalent functionalized carbon nanotubes were synthesized and characterized as effective electrocatalysts for proton exchange membrane fuel cells.[30] It was referred that non-covalent functionalization or wrapping by polyelectrolytes introduced large number of active sites uniformly on the surface of outer walls of CNTs without generating oxygenated functional groups or breaking the C–C bonds of the graphene sheets of the CNTs. Pt-based nanoparticles can then be uniformly dispersed on CNTs *via* self-assembly principle with significantly reduced agglomerates.[30] The well-defined geometry of outer wall surface of CNTs substantially promotes interconnectivity between Pt NPs, which leads to the significant increase in the grain boundaries between the NPs and thus active sites for fuel cell reactions.[31] The mechanism of the influence non-covalent functionalized CNTs on the electrocatalytic activity of Pt-based NPs, particularly at the atomic scale, is still unknown. Some authors proved the synergistic interaction between Pt nanoparticles and CNT.[32] Tian *et al.*[33] investigated the structural and electronic properties of Pt nanoparticles on various nitrogen, (N)-doped graphene and their interaction with O by density functional theory (DFT) calculations. These results indicated that N-doped graphenes not only stabilized the Pt clusters but also enhanced their catalytic performance in the oxygen reduction reaction. Pd–Pt nanostructures were synthesized by a sequential reduction using an ethylene glycol reduction method and deposited on carbon nanofibers.[34] The better performance in a single fuel cell was found with a Pd–Pt cathode than with a pure Pt commercial catalyst when both had the same loading of 0.5 mg of total metal per cm^2. Therefore this catalyst, synthesized using the described method, is a promising alternative to pure Pt catalyst as a lower-cost catalyst for the cathode of a PEMFC. Jager introduced the novel non-conventional microporous–mesoporous carbide derived carbon powder, synthesized from molybdenum carbide (Mo_2C) at 750 °C using the high-temperature chlorination method, and applied it as an electrocatalyst support for oxygen reduction.[35] This catalyst showed noticeably higher activity expressed as the shift of half-wave potential ($\Delta E_{1/2} \sim 50$ mV) explained by the optimized hierarchical microporous/mesoporous electrode structure.

All above discussed literature results showed the advantages of platinum nanoparticle catalysts deposited on different types of carbon based supports. Although carbon based materials possess many desirable properties, such as high surface area, high conductivity and relatively low cost and easy synthesis, the large scale commercialization is limited by insufficient stability, especially at high positive potential values (1.4 V *vs.* RHE and

higher). Degradation of the fuel cells catalyst during exposure to high anodic potentials has been already mentioned.[8,9] Accelerated durability tests (ADTs) were carried out for a carbon-supported platinum catalyst using a rotating disk electrode at various rotation rates for various catalyst loadings by Nagai *et al.*[36] The loss of the normalized ECSA increased with increasing the rotation rate and/or decreasing the catalyst loading. This analysis showed that the reciprocal of the normalized ECSA loss rate linearly increased with the increases in $\omega^{-1/2}$ and the catalyst loading, as it was presented in Fig. 2. These results suggested that ECSA loss in ADTs is significantly affected by Pt ion diffusion in the electrolyte.

An *in situ* electrochemical system for monitoring sub-monolayer dissolution of Pt under potential cycling was successfully established by Wang *et al.*[37] The amount of dissolved Pt^{2+} was calculated using collector current (IC) and was confirmed by *ex situ* inductively coupled plasma mass spectrometry. The amount of Pt^{2+} and Pt^{4+} dissolved in different potential regions during potential cycling was quantified by IC for the first time. The mechanism of Pt dissolution under potential cycling in 0.5 M H_2SO_4 was proposed.[37] Dhanushkodi *et al.*[38] established a novel method to characterize durability of carbon supported platinum nanocatalysts in membrane electrode assembly. It was shown that during the accelerate stability testing (AST) the variations operating parameters (*e.g.*, relative humidity, temperature and pressure), influenced the Pt dissolution rates and kinetic losses across the segmented cell. The Pt dissolution from the catalyst layer is shown to be non-homogenous during the AST *via* spatially resolved polarization resistance, kinetic polarization loss and the distance of the Pt band. Li *et al.*[39] developed a one-dimensional model and studied platinum degradation and the subsequent electrochemical surface area (ECA) loss in the cathode catalyst layer (CL) of polymer electrolyte fuel cells (PEFCs). The model includes two mechanisms of Pt degradation: Ostwald ripening on carbon support and Pt dissolution–re-precipitation through the ionomer phase. Impact of $H_2|N_2$ or $H_2|$air operation, operating temperature, and relative humidity on Pt degradation during voltage cycling was explored. It was shown that ECA loss is non-uniform across the cathode CL with a zone of exacerbated Pt degradation and hence much lower ECA found near the membrane. This non-uniform Pt degradation is caused by consumption of Pt ions by hydrogen crossover in both $H_2|N_2$ and $H_2|$air systems. Improved performance of nitrogen-modified carbon supports for direct methanol fuel cell (DMFC) applications was referred by Olson *et al.*[40] The nitrogen-ion implantation in high surface area carbon supports caused superior catalyst particle stability and performance as compared to industry standards. Specifically, results indicate a higher retention of metal catalyst surface area and electrochemical activity after accelerated electrochemical degradation testing.

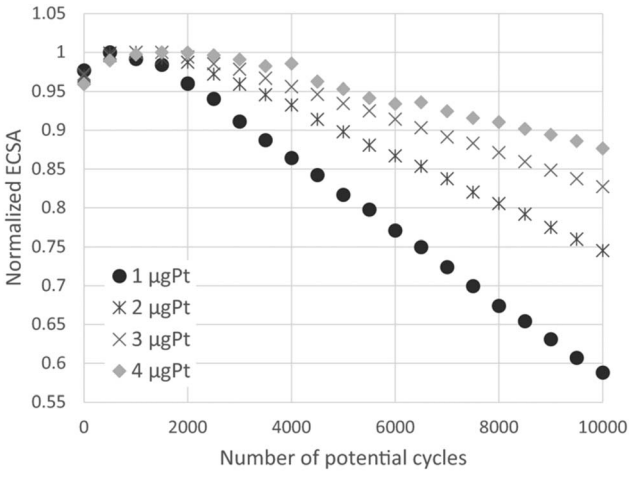

Fig. 2 The normalized ECSA as a function of the potential cycles at 400 rpm for various catalysts loadings. The normalization is based on the maximum ECSA during the ADT. Reprinted with permission of The Electrochemical Society in ref. 36.

3. Pt catalysts at metal oxide based supports for PEMFCs

In the previous section the contemporary research related to carbon based support was presented. It was clearly shown that carbon supported nanocatalysts suffer from serious problems caused by instability under accelerated stability testing, simulating real fuel cell operating conditions. This fact implies demand to introduce novel support materials, to overcome disadvantages of carbon based ones. For this purpose several types of metal oxide based supports have been studied and promising results were referred. The common required properties which make metal oxide suitable for platinum nanoparticles support are: high chemical stability in acid and alkaline electrolytes; high corrosion resistance-metal oxides should be electrochemically stable at fuel cells operating conditions; good electronic conductivity, to enable ultralow platinum loading; good proton conductivity; high surface area to enable high utilization of noble metal particles. The survey presenting the most often used oxide based supports for low temperature fuel cells application will be presented below.

3.1. Molybdenum oxide supported Pt nanocatalysts

Investigations of molybdenum oxides have attracted remarkable researchers' interest for prospective fuel cells application. It is well known that molybdenum forms five Magneli phases oxide, with composition between MoO_2 and MoO_3. The presence of molybdenum oxide can significantly enhance activity and stability of noble metal catalysts by the strong metal support interaction, as well as by the formation of hydrogen molybdenum bronze.[41] Chen *et al.*[42] referred hydrogen molybdenum bronze formation and revealed hydrogen spillover on MoO_3 in the presence of platinum. Elezovic *et al.*[43,44] synthesized MoO_x–PtC catalyst by the polyole method combined by MoO_x post-deposition and characterized it for oxygen reduction and methanol oxidation reactions. Thermal treatment of this catalyst caused the loss in active surface area for about 26%, which was explained with oxide particle agglomeration in small three-dimensional islands on the neighboring Pt particles, decreasing

the active surface area. The increase in catalytic activity for ORR on MoO_x–Pt/C, in comparison with Pt/C catalyst, was explained by synergetic effects due to the formation of the interface between the platinum and oxide materials and by spillover due to the surface diffusion of oxygen reaction intermediates. The catalytic effect in oxidation of methanol is achieved only under potentiodynamic conditions, when poisoning species have no enough time to develop fully. Mixed valence state of molybdenum oxide was referred by Wang *et al.*,[45] as well. They prepared Pt/MoO_x catalysts by electrodeposition method and proposed promotion mechanism of MoO_x for methanol oxidation reaction, causing removal of the adsorbed CO poisons at lower potentials. Justin *et al.* applied microwave assisted polyol method to incorporate MoO_3 into Vulcan XC 72 particles.[46] This catalyst exhibited high activity for methanol oxidation, as well as better stability than carbon supported one. The significant improvement in electrocatalytic activity and stability for the MOR was attributed to the strong metal-support interaction between Pt and MoO_3, and the formation of hydrogen molybdenum bronze during the CV measurements, which reduces the CO poisoning of Pt catalysts. Papageorgopoulos *et al.*[47] investigated the effect of the inclusion of Mo, Nb and Ta in Pt and PtRu carbon supported anode electrocatalysts on CO tolerance. Performed fuel cell tests demonstrated that while all the prepared catalysts exhibited enhanced performance compared to Pt/C, only the addition of a relatively small amount of Mo to PtRu results in a higher activity, in the presence of carbon monoxide. Ioroi *et al.*[48] prepared carbon-supported Pt/Mo-oxide catalysts and examined the reformate tolerances of Pt/MoO_x/C and conventional carbon supported anodes. Fuel cell performance was evaluated under various reformate compositions and operating conditions, and the CO concentrations at the anode outlet were analyzed simultaneously using on-line gas chromatography. Pt/MoO_x showed better CO tolerance than PtRu with CO (80 ppm)/H_2 mixtures, especially at higher fuel utilization conditions, which is mainly due to the higher catalytic activity of Pt/MoO_x for the water-gas shift (WGS) reaction and electro-oxidation of CO. Ioroi *et al.*[49] tested carbon-supported Pt/MoO_x catalysts for the oxidation of CO contaminated H_2, based on the fuel cell performance in PEFC single cell arrangements. Based on the XRD pattern and XPS measurements of the prepared catalysts, it was found that the deposited MoO_x exists as an amorphous oxide phase. The MoO_x phase shows a redox peak at around 0.45 V, which was revealed by the cyclic voltammogram of the Pt = MoO_x = C in sulfuric acid solution. The PEFC performance of the cell with Pt = MoO_x = C was improved under 100 ppm CO-contaminated H_2 conditions compared to the Pt/C catalyst, and was almost comparable to the PtRu(1 : 1)/C catalyst. Yan *et al.*[50] synthesized the single molybdenum oxide (MoO_2) crystals 5 nm in diameter on carbon, (denoted as C–MoO_2) and tested structures, morphologies, chemical and electrocatalytic performances of the Pt nanoparticles supported on C–MoO_2 (denoted as Pt/C–MoO_2). High activity and stability for oxygen reduction was proven. A mass activity of 187.4 mA mg^{-1} Pt at 0.9 V is obtained for ORR, which is much higher than that on commercial Pt/C (TKK) electrocatalyst (98.4 mA mg^{-1} Pt). Furthermore, the electrochemical stability of Pt/C–MoO_2 was higher than that of Pt/C. The origin of the improvement in catalytic activity was attributed to the synergistic or promotion effect of MoO_2 on Pt.

3.2. Tungsten based supports for Pt nanocatalysts

Tungsten typically with oxygen forms stoichiometric tungsten trioxide, WO_3, and lower non-stoichiometric oxides, WO_x, where $2 < x < 3$. Apart of WO_3, only three stable tungsten oxides exist: β-oxide ($W_{20}O_{58}$), γ-oxide ($W_{18}O_{49}$), and δ-oxide (WO_2).[51] All other compounds are either metastable or consist of solid solutions of these three phases and WO_3. WO_3 is an n-type semiconductor with a reported band gap of about 2.6 to 2.8 eV.[52] WO_3 is insoluble in acid, while WO_2 is soluble in acid and alkaline solution.[53] In aqueous alkaline solutions WO_3 forms tungstate ions, WO_4^{2-}. Tungsten carbides (W_2C and WC) are some of the hardest carbides, with melting point of 2770 °C for WC and 2780 °C for W_2C. WC is an efficient electrical conductor, but W_2C is less conductive. Tungsten carbide, as low cost alternative to bulk precious metal catalysts, is an excellent candidate support material for Pt monolayer, leading to good adhesion and utilizing the lowest possible Pt loading.[54] Electrochemical stability of tungsten and tungsten carbide over wide pH and potential ranges have been studied and both materials showed promise as an anode, while operating within the region of passivation, and as a cathode, across the entire pH range.[55]

Tungsten-based materials can play different roles in fuel cell systems. They are the only compounds which can be used as catalysts, co-catalysts, catalyst supports and electrolytes in different types of fuels cells. In particular, tungsten-based materials fulfill the requirements for their use as thermally stable carbon-alternative catalyst supports and Nafion®-alternative proton conducting electrolytes in fuel cells operating at intermediate temperature.[56] Weigert *et al.* studied electrochemical behavior of tungsten carbide (WC) and platinum-modified WC as alternative DMFC electrocatalyst.[57] Evidence of improved anode kinetics was observed by increasing the fuel concentration and operating temperature, particularly at 70 °C. It was evident that the most prominent limiting factor for the performance of membrane electrode assembly, prepared with this material, is the low surface area of the anode catalyst. Wang *et al.*[58] prepared the high surface area (256 m^2 g^{-1}) tungsten carbide microspheres (TCMSs) by a simple hydrothermal method and studied performance of Pt electrocatalyst supported on the as-prepared TCMSs towards the oxygen reduction reaction (ORR). XRD results revealed presence both W_2C and WC, while W_2C exists as the main phase. It was found that the Pt particles are uniformly dispersed on the supports, while the corresponding average particle size was 3.7, 4.1 and 4.3 nm for Pt/C, Pt/CMSs and Pt/TCMSs, respectively. It was also found that in terms of ORR onset potential and mass activity, the Pt/TCMSs catalyst exhibits superior performance to that of Pt/CMSs and Pt/C. Catalytic activity improvement was attributed to higher electrochemical surface area (ESA), as well as to the synergistic effect between Pt and tungsten carbides. Hara *et al.*[59] synthesized WC based support by the carburizing of tungsten nitrides

(W_2N) and tungsten sulfides (WS_2) as precursors from different starting materials. Binary Pt–WC catalysts were prepared, with greatly improved performance by choosing a suitable WC and modifying the preparative method. As a result, it turned out that the mass activity of the Pt–WC catalyst system was superior to the current commercial Pt catalyst although only one-tenth the amount of Pt metal was used. It is thought that there is a synergistic effect between Pt and WC in terms of activity, leading to a drastic reduction in the use of Pt metal. Zhu *et al.*[60] modified mesoporous carbon with tungsten carbides by the carbothermal hydrogen reduction of a layer of chemisorbed 1 : 12 phospho tungstic anions ($PW_{12}O_{40}^{3-}$). Depending on the temperature of carbothermal treatment, different tungsten species, *i.e.*, W, W_2C, WC, were formed on the carbon matrix. Uniform dispersion of Pt nanoparticles (1–6 nm) was achieved on the surfaces of both mesoporous carbon and tungsten carbide-modified mesoporous carbon. Pt nanoparticles supported on mesoporous carbons modified with tungsten carbide (Pt/WC–C) exhibit enhanced electrocatalytic activities relative to the control, in which mesoporous carbons without carbide modification were directly used as a support (Pt/C). In addition, both enhanced thermal stability and good electrochemical stability were observed for the Pt/WC–C electrocatalyst.[60] The thermal and electrochemical stability of tungsten carbide (WC), with and without a catalyst dispersed on it, have been investigated to evaluate the potential suitability of the material as an oxidation-resistant catalyst support.[61] Electrochemical testing was performed by applying oxidation cycles between +0.6 V and +1.8 V to the support-catalyst material combinations and monitoring the activity of the supported catalyst over 100 oxidation cycles. The electrochemical activity of the Pt/WC remained nearly constant over 100 accelerated oxidation cycles, while the activity of Pt/C was almost completely lost after only approximately 20 oxidation cycles. However, the initial activity of the Pt/WC supported catalyst is much lower than that of Pt/C at comparable volumetric catalyst loadings, indicating that higher surface area WC supports and better platinum dispersion techniques are still required in order to enhance the catalyst layer activity.[61] Shengsheng *et al.* investigated oxidation resistance of tungsten carbide a catalysts support for proton exchange membrane fuel cells.[62] The measurements described above showed that the Pt/W_xC_y catalyst possessed higher stability than the traditional Pt/C during the oxidation tolerance test owing to the excellent performance of the new support. Improvement of the surface area and rationalization of the pore distribution should be made to enhance the applicability of the tungsten carbide support. Mellinger *et al.*[63] tested tungsten carbide and Pt-modified WC as CO-tolerant electrocatalysts as compared to pure Pt. The binding energies of CO, estimated from the desorption temperatures in the TPD measurements, are significantly lower on WC and Pt/WC surfaces than on pure Pt, indicating that the former two surfaces should be more CO-tolerant than Pt under typical PEMFC operating temperatures. The combination of low coverages of Pt with WC results in a synergistic effect for the oxidation of CO, leading to a higher activity than Pt and higher stability than WC. The promising properties of Pt/WC suggest the possibility of utilizing these materials either as CO-tolerant electrocatalysts or as purification catalysts to oxidize CO in the fuel feed stream. Weigert *et al.*[64] examined the electrochemical stability of tungsten carbide (WC), Pt-modified WC, molybdenum carbide (Mo_2C), and Pt-modified Mo_2C using an *in situ* electrochemical half-cell in combination with X-ray photoelectron spectroscopy (XPS). At potentials higher than ~0.8 V, WC oxidizes irreversibly into W_xO_y species as confirmed by the CV and XPS measurements. The deposition of submonolayer coverage of Pt on the WC surface increased the region of stability of WC, extending the onset of catalysts oxidation to ~1.0 V (NHE). Therefore, Pt-modified WC can be a promising alternative electrocatalyst. Shen *et al.*[65] introduced intermittent microwave heating (IMH) method for preparation of nanosized tungsten carbides. It produced WC with the average particle size of 21.4 nm at the procedure of 15 s-on and 15 s-off for 20 times, however, the particle size increased to 35.7 nm by CMH method for 5 min. The pure WC was obtained by post-treating the sample in NaOH solution, which gave the better performance as support. The nanosized WC was used as support for the Pt nanoparticles (Pt–WC/C (IMH)) for alcohol oxidation and oxygen reduction. It was proved that the Pt–WC/C (IMH) electrocatalysts gave the better performance than that prepared by CMH method (Pt–WC/C (CMH)) or Pt/C electrocatalysts in terms of the activity and CO-tolerance. Esposito and Chen[66] discussed possibility to deposit monolayer platinum supported on tungsten carbides as low-cost electrocatalysts (ML Pt–WC). Density functional theory (DFT) calculations and experimental measurements indicate that the ML Pt–WC surface exhibits chemical and electronic properties that are very similar to bulk Pt for simple reactions such as the hydrogen evolution reaction, although deviation in behavior is observed for more complex reactions such as the electrooxidation of methanol. However, the challenges associated with the synthesis of such structures in a manner that can easily be scaled up in a cost-effective process are numerous. Ganesan *et al.*[67] synthesized mesoporous WC with hexagonal crystal structure by a surfactant-assisted polymer method. A new electrocatalyst composed of a small amount of Pt supported on the mesoporous WC exhibited higher activity for electrooxidation of methanol than microporous Pt/WC or Pt/W_2C as well as commercial Pt–Ru (1 : 1)/C catalysts. Xu *et al.*[68] referred improving sulfur tolerance of noble metal catalysts by tungsten oxide-induced effects. WO_x is adopted for the first time to modify such noble metal catalysts with an aim of acquiring excellent sulfur tolerance, due to its unique nature with hydrophilicity, redox couple in lower valence, as well as proton spillover effect. A series of WO_x–Pt/C catalysts with various contents of tungsten oxide from 1 to 50 wt% were synthesized and compared to conventional Pt/C catalysts toward sulfur resistance using cyclic voltammetry (CV), as well as rotating ring disk electrode (RRDE) methods. Moreover, the higher catalytic activity of WO_x–Pt/C toward oxygen reduction reaction (ORR) is revealed in comparison with Pt/C after both were poisoned by SO_x where the electron transfer number of the former is closer to four-electron than that of the latter. The electronic interaction between Pt and WO_x is evidently confirmed by X-ray photoelectron spectroscopy analysis and strongly suggested as

the crucial factor for the ORR enhancement. Elezovic *et al.*[69–71] synthesized and characterized platinum nanocatalysts on two tungsten based supports as the catalysts for oxygen reduction reaction in acid and alkaline solutions. Tungsten based support assigned WC_{ctabr} has been synthesized by polycondensation of resorcinol and formaldehyde in the presence of CTABr surfactant. Support assigned WC_{WO_3} was synthesized from resorcinol/formaldehyde gel, using WO_3 nanoparticles as starting material. Supporting materials have been characterized by BET (Brunauer, Emmett and Teller) technique and determined values of surface area were 80 $m^2 g^{-1}$ for WC_{ctabr} and 175 $m^2 g^{-1}$ for WC_{WO_3}. These catalysts exhibited better catalytic activity, expressed in terms of kinetic current density per real surface area at the constant potential and better stability, in comparison with Pt/C catalyst. Core–shell structure of WC_{ctabr}, containing W core and WC shell about 2–5 nm of thickness was confirmed by HRTEM technique (presented in Fig. 3).

EDS analysis confirmed that shell was mixture of tungsten oxide and tungsten carbide. EELS have been performed as complementary technique to EDS spectroscopy, to confirm core–shell structure.

It is interesting to note that the existence of the Pt particles size lower than 2 nm, even clusters of Pt atoms were obtained (Fig. 4). This high resolution TEM image shows one-dimensional lattice fringes belonging to the (1 1 1) Pt plane (black square upper, Fig. 4b). Presence of tungsten particles oriented close to 100 zone axis is also indicated (black square lower, Fig. 4b).

Garcia *et al.*[72] investigated the activity of Pt catalysts dispersed on tungsten carbide (WC) prepared with a high surface area carbon with two different WC/C ratios for the oxygen reduction reaction (ORR) in alkaline electrolyte. The PtWC-based catalysts show higher activity for the ORR compared to Pt/C, also involving a transfer of 4 electrons per oxygen molecule. CV and X-ray absorption near edge structure spectroscopy (XANES) results for the PtWC-based materials indicate weaker Pt–OH_x interaction in these materials, resulting in a lower Pt-oxide coverage and explaining the increased rate of the ORR, as compared to Pt/C. Yan *et al.*[73] presented an ion exchange route to produce WO_3 nanobars as Pt electrocatalyst promoter for oxygen reduction reaction. Pt nanoparticles were supported on the C–WO_3 composites (Pt/C–WO_3) and used as electrocatalyst for ORR. The results showed that WO_3 with moderate concentration could give the best promotion effect on Pt supported electrocatalyst. A typical Pt/C–WO_3 (0.05) electrocatalyst gives the kinetic mass current of 174.6 mA mg^{-1} Pt, which is much higher than that of commercial Pt/C electrocatalyst (98.6 mA mg^{-1} Pt) for ORR at the same Pt loadings. Moreover, the electrochemical stability of Pt/C–WO_3 was excellent. The higher catalytic activity and chemical stability may be due to the promotion effect of WO_3 nanobars on Pt and the strong interaction force between WO_3 and Pt respectively. Li *et al.*[74] studied sub-stoichiometric tungsten oxide $W_{18}O_{49}$ as a support for a Pt catalyst. Pt/$W_{18}O_{49}$, achieved higher catalytic

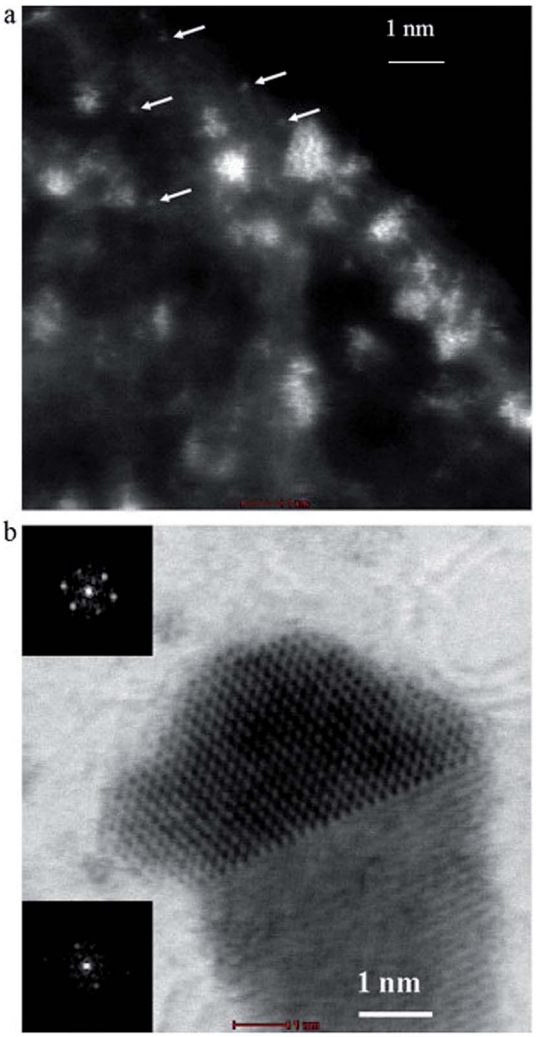

Fig. 4 STEM images of the Pt/WC catalyst the smallest particles of Pt lower than 2 nm as clusters of Pt atoms. The arrows indicate individual Pt atoms, the indication Pt particle nucleated on WC support. Reprinted from Electrochimica Acta in ref. 70, with permission of Elsevier.

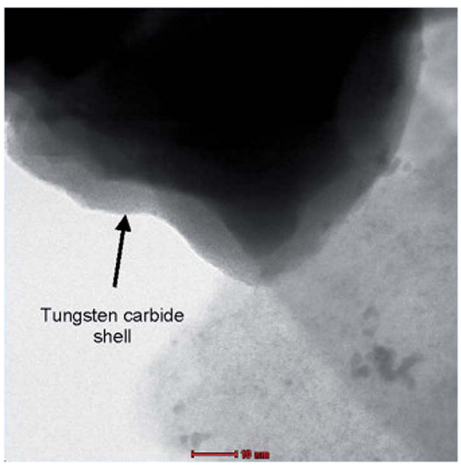

Fig. 3 High resolution TEM micrograph of WCctabr support. Reprinted from Applied Catalysis B: Environmental in ref. 69, with permission of Elsevier.

activity, antipoisoning properties and stability than the commercial Pt-black and Pt/C catalysts. XPS results revealed a strong metal-support interaction between Pt and the $W_{18}O_{49}$. In addition, two valence states of W (W^{5+} and W^{6+}) were found to co-exist in $W_{18}O_{49}$, which may promote hydrogen spillover and oxygen buffering effects. These effects contributed to the improvement of the poisoning tolerance and the catalytic activity. Xiong *et al.*[75] synthesized tungsten carbide support by the template of amorphous carbon microspheres (CMS), which is prepared by a hydrothermal synthesis process using glucose as the carbon precursor. The WC/CMS support is characterized by XRD, SEM, and BET. Pt nanoparticles were loaded on the WC/CMS support and Pt/WC/CMS catalyst was formed. The as-prepared Pt/WC/CMS showed higher electrocatalytic activity and anti-poisoning ability over Pt/C for the electrooxidation of ethanol. The rate constant of oxygen reduction reaction for Pt/WC/CMS is twice as high as that of Pt/C, indicating the synergetic effects between the Pt and the WC support. Furthermore, Pt/WC/CMS exhibits much higher stability for the ethanol electro-oxidation than Pt/C, which can be attributed to the high stability of WC support.

3.3. Titanium oxide based supports for Pt nanocatalysts

Titanium based oxides (commercially called Ebonex), with the integer formula Ti_nO_{2n-1} ($4 < n < 10$), and between them the most pronounced their first two oxides, *i.e.* Ti_4O_7 and Ti_5O_9, have attracted a lot of attention as new catalyst supports.[76,77] These oxides exhibit electrical conductivity and chemical stability at room temperature similar to these of carbon and graphite. The corrosion stability of these oxides in aqueous electrolytes is very high and they do not form hydrides in contact with hydrogen. All of that make them suitable as a support. Investigation of ORR at Ebonex supported Pt nanoparticles in 0.1 mol dm^{-3} NaOH solutions, revealed similar catalytic activity to polycrystalline Pt.[77] High catalytic activity towards oxygen evolution at PtCo referred by Slavcheva *et al.*[78] is related to the formation of surface oxides and electronic interactions between the metallic components of the catalyst and the supportive Ebonex. However, the problem with Ebonex powder was its very low specific surface area.[78] Sasaki *et al.*[79] demonstrated that niobium oxide nanoparticles could be adequate support for Pt, reducing at the same time the noble-metal contents of catalyst for oxygen reduction. Since niobium oxides have excellent chemical stability they could diminish the problems of substrate oxidation and corrosion degradation. It has also been reported that, by doping titania with pentavalent niobium ions, these ions get into the anatase titanium oxide crystalline structure preventing its phase transformation to rutile. This effect has been attributed to the extra valence of niobium ions, reducing oxygen vacancies in anatase phase and inhibiting the transformation to rutile. Park and Seul[80] referred that $NbTiO_2$ supported Pt catalyst showed an excellent catalytic activity for ORR in acid solution, mainly due to the good dispersion of Pt on $NbTiO_2$. Elezovic *et al.*[81,82] synthesized Nb doped TiO_2 support by modified acid-catalyzed sol–gel procedure in non-aqueous medium. The catalytic activity and stability of Pt nanocatalysts synthesized onto this support were studied in both acid and alkaline solutions. This Nb–TiO_2 (0.5% Nb) supported Pt nanocatalyst exhibited higher catalytic activity for ORR in acid solution, if compared with carbon supported Pt catalyst.[81] Synthesized support surface area (91 m^2 g^{-1}) was much higher comparing with very low specific surface area of sub-stoichiometric titanium oxides as supporting material. Although the catalytic activities in alkaline solution were similar, the importance of new synthesized Nb doped TiO_2 support, should be emphasized, as it was proved to be more stable than carbon based support.[82] Xia *et al.* prepared high-stability Pt electrocatalysts using hierarchical carbon nanotubes, CNT@TiO_2 structures composed of TiO_2 nanosheets grafted on the CNT backbone as the support. The as-prepared Pt/CNT@TiO_2 electrocatalysts manifest high electrocatalytic activity with greatly improved stability compared to conventional CNT or carbon black supported Pt electrocatalysts.[83] Shi *et al.*[84] achieved two times higher activity and three times higher stability in methanol oxidation reaction, a 0.12 V negative shift of the CO oxidation peak potential, and a 0.07 V positive shift of the oxygen reaction potential compared to Pt nanoparticles on pristine TiO_2 support by tuning the electronic structure of the titanium oxide support of Pt nanoparticle catalysts. To explain the observed trends, an electronic structure model of Pt/TiO_x electrocatalyst systems was introduced that shows an enhancement of the electrochemical activity of the Pt nanoparticles when the Fermi level of the support material is close to the Pt Fermi level and the redox potential of the reaction so that to facilitate electron transfer among the electrode, the Pt nanoparticles, and the electrolyte. Kumar and Ramani[85] synthesized tantalum (Ta) modified TiO_2 using a sol–gel procedure and evaluated for use as an electrocatalyst support. Pt supported on $Ta_{0.3}Ti_{0.7}O_2$ was synthesized for further evaluation. The durability and catalytic activity of this material was measured and benchmarked against the state-of-the-art 46% Pt/C TKK electrocatalyst as well as 20% Pt/C catalyst prepared in-house. $Ta_{0.3}Ti_{0.7}O_2$ exhibited an order of magnitude higher electrochemical stability than the benchmark carbon material when examined using an aggressive accelerated test protocol that simulated 10 000 start-up and shut-down cycles (support stability test protocol: 1.0–1.5 V *vs.* RHE at a scan rate of 500 mV s^{-1} in a 0.1 M$HClO_4$ electrolyte at 25 °C). 20% Pt/$Ta_{0.3}Ti_{0.7}O_2$ also demonstrated greater electrochemical stability than both Pt/C catalysts, as estimated using the load cycling protocol, showing a 35% *vs.* a 44–47% loss in ECSA over 10 000 load cycles (load cycling test protocol: 0.6–0.95 V *vs.* RHE with a dwell time of 3 s at either potentials in a 0.1 M $HClO_4$ electrolyte at 25 °C). Siracusano *et al.*[86] synthesized bare and Nb and Ta doped Ti-oxides by using various synthesis routes and investigated in terms of structure, morphology and electrochemical properties for application as catalyst supports in low temperature fuel cells. Non-carbonaceous supports prepared by colloidal procedures showed an excellent corrosion resistance, at least one order of magnitude better than Ketjenblack EC used as reference. The use of an oxide support appears promising to strongly improve the cathode catalyst stability especially under critical conditions that may occur in a fuel cell whereas suitable

performance can be obtained by tailoring the catalyst preparation conditions. Zhang *et al.*[87] demonstrated method for preparation of Pt/TiO_2 nanotube arrays by H_2 reduction. The effects of the reduction atmospheres and temperatures on Pt catalysts preparation were investigated. The well dispersion of Pt catalysts supported onto the TiO_2 nanotube array exhibited favorable electrochemical performance and excellent durability. Tiido *et al.*[88] prepared nano-sized Pt catalyst supported onto titanium dioxide functionalized graphene nanosheets (TiO_2-FGSs) using the polyol method and utilized for a catalyst activity investigation toward the oxygen reduction reaction (ORR). The catalyst exhibited a relatively high electrocatalytic activity for the four-electron reduction of oxygen to water. Huang *et al.*[89] dispersed Pt nanoparticles into mesoporous TiO_2 thin films fabricated by a facile electro-chemical deposition method and tested it as electro-catalysts for oxygen reduction reaction. The XPS studies confirmed that the TiO_2 support had a strong influence on the electronic structure of the platinum particles deposited, which in turn affected the composite's activity. The electrochemical deposition method can be a generally used approach to the preparation of metal NPs into oxide nanocrystalline mesoporous solid thin film, which has potential applications in fuel cell. Meenakshi *et al.*[90] developed a new carbon supported HT–Pt–TiO_2 composite catalyst comprising Pt and Ti in varying atomic ratio, namely 1 : 1, 2 : 1 and 3 : 1. ORR studies in the presence and absence of ethanol on HT–Pt–TiO_2/C catalyst containing Pt and Ti in varying atomic ratio show that HT–Pt–TiO_2 (2 : 1)/C exhibits higher ORR activity. DEFC employing HT–Pt–TiO_2 (2 : 1)/C as cathode catalyst exhibits better performance than that with Pt/C. Therefore, HT–Pt–TiO_2/C catalyst is a good cathode catalyst for ethanol tolerant-oxygen-reduction reaction in direct ethanol fuel cells. Savych *et al.*[91] synthesized TiO_2 nanofibres (TNF) and carbon nanofibres (CNF) by electrospinning/calcination. Electronic conductivity of TNF was improved by doping and specific thermal treatments. Pt/TNF showed superior electrochemical stability compared to Pt/CNF. Rigdon and Huang[92] prepared carbon monoxide tolerant platinum electrocatalysts on niobium doped titania and carbon nanotube composite supports. Bifunctional reactivity of platinum can be improved by the addition of select metal oxides to the surface of multi-wall carbon nanotube supports. Specifically, titania was donor doped with niobium in construction of stable electrocatalysts used in anodes with the best tolerance to 100 ppm carbon monoxide during hydrogen oxidation. Ruiz-Camacho *et al.*[93] synthesized Pt nanoparticles by chemical vapor deposition on carbon and TiO_2–C substrates. Significant differences in the electrochemical results and alcohols tolerance are observed in the samples prepared in comparison whit Pt/C commercial catalyst. The methanol tolerance of the catalysts synthesized was higher compared to the ethanol tolerance. The electrochemical activity of Pt/TiO_2–C catalyst prepared with TiO_2 rutile phase was not affected by the presence of alcohols in comparison with Pt/C samples. It is explained by the thermal treatment over Pt/TiO_2–C during the synthesis process that produces a synergetic effect caused by the formation of the interface between the platinum and oxide materials where titanium oxide acts as a protecting agent of platinum nanoparticles. Jukk *et al.*[94] prepared Pt nanoparticle-titanium dioxide/multi-walled carbon nanotube (Pt–TiO_2/MWCNT) materials by combining chemical vapour deposition (CVD), atomic layer deposition (ALD) and magnetron sputtering techniques. It was proven that incorporating TiO_2 into the structure of fuel cell catalyst supports can improve the electrocatalytic activity of Pt nanoparticles towards the ORR. The specific activity of Pt–TiO_2/MWCNT catalysts for oxygen reduction was slightly higher than that of commercial Pt/C in acid media. The prepared composite materials showed also a substantial electrocatalytic activity for ORR in alkaline solution. Liu *et al.*[95] studied the oxygen reduction reaction (ORR) activity of $Pt_{90}Au_{10}$/C, promoted by TiO_x modification. After accelerated durability testing, the ORR activity of PtAu/C with 3 wt% TiO_x is 2.7 times higher than that of the Pt/C, attributed to the suboxide formation and moderate surface Pt–Au ratio. Li *et al.*[96] synthesized a new type of SnO_2–TiO_2 solid solution ($Ti_xSn_{1-x}O_2$) support was prepared *via* a solvothermal method with substitution of Ti_4þ by Sn_4þ in the TiO_2 lattice. Furthermore, the $Ti_xSn_{1-x}O_2$ was combined with conventional carbon black (Vulcan XC-72) to prepare a hybrid support ($Ti_xSn_{1-x}O_2$-eC) for depositing Pt nanoparticles. The ratios of Sn *vs.* Ti in the solid-solution and $Ti_xSn_{1-x}O_2$ *vs.* XC-72 were systematically optimized in terms of their performance as supports for methanol oxidation. The enhanced activity for Pt supported on $Ti_{0.9}Sn_{0.1}O_2$–C is explained by high content of OH group on $Ti_{0.9}Sn_{0.1}O_2$ along with the strengthened metal supports interactions. Both promote the oxidation of poisoning CO absorbed on Pt active sites. Odetola *et al.*[97] referred enhanced activity and stability of Pt/TiO_2/carbon fuel cell electrocatalyst prepared using a glucose modifier. Higher ORR activity achieved when TiO_2 was prepared with glucose doped carbon. Catalyst prepared with TiO_2 showed slower rates of Pt dissolution/agglomeration compared to Pt/C. Sui *et al.*[98] reported a rapid method to synthesize titania nanotubes as the support for a Pt-based catalyst. The titania nanotubes can be obtained during 1200 s in an ethylene glycol system by the anodization method. Pt nanoparticles were successfully deposited on a mixture of carbon and as prepared TiO_2 nanotubes by a microwave-assisted polyol process. These studies have shown that the Pt/C–TNTs–EG catalyst served as a highly efficient catalyst for the methanol electrooxidation reaction with better activity and durability than the commercial Pt/C. The enhanced performance could be attributed to the metal-support interactions and hydrogen spillover effect between the Pt nanoparticles and titania, the high corrosion resistance of titania, the good electronic conductivity due to the addition of carbon, and the good dispersion of the Pt nanoparticles on the titania nanotubes. The results reported herein suggest that titania nanotubes obtained by anodization have potential for applications in the future. Shintani *et al.*[99] introduced novel strategy to mitigate cathode catalyst degradation during air/air startup cycling *via* the atmospheric resistive switching mechanism of a hydrogen anode with a platinum catalyst supported on tantalum-doped titanium dioxide. It was shown that cathode degradation during startup was reduced by use of $Pt/Ti_{0.9}Ta_{0.1}O_{2-\delta}$ anode. The membrane electrode assembly (MEA) with the Pt/

$Ti_{0.9}Ta_{0.1}O_{2-\delta}$ anode showed higher performance than the MEA with the Pt/GCB anode after the air/air startup cycling (presented in Fig. 5).

They concluded that the reverse current can be reduced by decreasing the ORR current generation on the Pt/Ta–TiO_2 anode due to its high resistivity in air.

Elezovic *et al.*[100,101] synthesized ruthenium doped TiO_2 by hydrazine reduction method and apply it as a support for Pt nanoparticles. XRD analysis revealed mainly presence of anatase TiO_2 phase and some peaks belonging to rutile TiO_2. This new catalyst exhibited remarkable enhanced catalytic activity for oxygen reduction reaction in acid solution, compared to Pt/C. Increased catalytic activity of the Pt/$Ru_{0.7}Ti_{0.3}O_2$ catalyst could be explained by effect of the support on the electronic structure of the catalyst due to the so called Strong Catalyst Support Interaction (SCSI). The hypo-d-electron transition metal oxides, such as TiO_2, exhibit strong metal support interaction (SMSI) [100], which can improve the activity of the Pt catalyst towards the ORR. The modification of the electronic structure of Pt nanoparticles by interaction with the oxide interface results in a change in the adsorption characteristics of Pt on Ru–TiO_2 support.

3.4. Tin oxide based supports for Pt nanocatalysts

SnO_2, a broadband oxide semiconductor, with relatively high electronic conductivity, could be considered as a promising carbon-free catalyst support. The main advantages of tin oxide if compared to titanium based oxides are lower price of Sn than Ti and higher electrical conductivity. Santos *et al.*[102] electrodeposited platinum micro particles on SnO_2 thin films in order to verify the application of this system as a catalyst for the electrooxidation of methanol. The chronoamperometric results showed that the current values obtained for the electrooxidation of methanol were up to 10 times higher than the current values obtained with platinized platinum under the same conditions.

Saha *et al.*[103] prepared electrode by electrochemical deposition of platinum nanoparticles onto the surface of tin oxide SnO_2 nanowires (NW) directly grown on the carbon fibers of a carbon paper. High electrocatalytic activities of the Pt/SnO_2 NW/carbon paper composite electrode for both oxygen reduction reaction and methanol oxidation reaction have been achieved in comparison with standard Pt/C electrode. The higher electrocatalytic activities are attributed to the interaction of Pt nanoparticles with the SnO_2 NW supports, as well as the 3D composite electrode structure. Lee *et al.*[104] studied electrocatalytic activity and stability of Pt supported on Sb-doped SnO_2 nanoparticles (Pt/ATO) for direct alcohol fuel cells. The activities of the Pt/ATO for both MOR and EOR were greater than those of the Pt/C as the amount of loaded Pt decreased. These enhanced activities can be attributed to better dispersion of Pt particles on the ATO support, as well as to the effects of SnO_2 adjacent to Pt, such as the bifunctional effect and/or the electronic effect. Takasaki *et al.*[105] used SnO_2 as an alternative electrocatalyst support improving durability against voltage cycling up to a high potential, corresponding to the start-up and shut-down situation of polymer electrolyte fuel cell (PEFC) systems. Electrochemical surface area (ECSA) and oxygen reduction reaction (ORR) activity of Pt electrocatalysts as well as electrical conductivity of the electrocatalyst layers increase by doping of SnO_2 with Nb or Sb. The durability tests with voltage cycles between 0.9 and 1.3 V *versus* reversible hydrogen electrode (RHE) potential have revealed that the Pt electrocatalyst supported on SnO_2 (Pt/SnO_2) withstands 60 000 voltage cycles while maintaining its ECSA, which corresponds to a lifetime of more than 20 years with respect to the durability against voltage cycling (presented in Fig. 6).

Nanostructure, electrochemical properties and durability of carbon-free electrocatalysts, Pt/SnO_2, Pt/Nb–SnO_2, Pt/Al–SnO_2, were investigated by Takasaki *et al.*[106] ECSAs of the electrocatalysts using the SnO_2-based supports were lower than the ECSA of the conventional Pt/C. In comparison with Pt/SnO_2, Pt/$Sn_{0.95}Nb_{0.05}O_2$ exhibited slightly larger ECSA, whereas smaller ECSA was obtained for Pt/$Sn_{0.95}Al_{0.05}O_2$. Kinetic current density

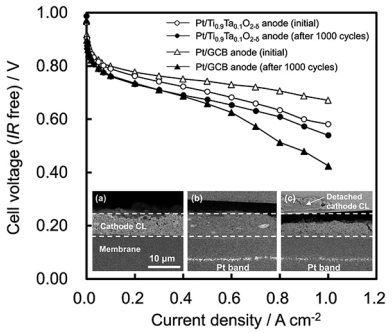

Fig. 5 IR-free H_2/air polarization curves of Pt/$Ti_{0.9}Ta_{0.1}O_{2-\delta}$ anode cell (circles) and Pt/GCB anode cell (triangles) at 65 °C and 100% RH, initially (open symbols) and after the air/air startup cycling (solid symbols); H_2 utilization 70%, oxygen utilization 40%, ambient pressure. The inset shows the cross-sectional SEM images of Pt/GCB cathode regions; for (a) the pristine MEA with Pt/GCB anode and the startup-tested MEAs with (b) Pt/$Ti_{0.9}Ta_{0.1}O_{2-\delta}$ anode and (c) Pt/GCB anode. Reprinted from Journal of Power Sources in ref. 99, with permission of Elsevier.

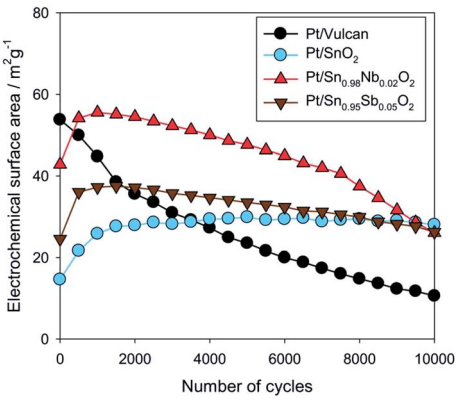

Fig. 6 (Color online) ECSA *vs.* number of cycles in the potential range from 0.9 V to 1.3 V RHE, up to 10 000 cycles. Reprinted from Journal of The Electrochemical Society in ref. 105, with permission of The Electrochemical Society.

of the electrocatalysts with the oxide supports was lower than that of Pt/C. Among the electrocatalysts examined, Pt/$Sn_{0.95}Nb_{0.05}O_2$ exhibited the highest kinetic current value. In the durability test in the high potential range (0.6–1.3 VRHE) by CV, while the ECSA of Pt/C rapidly decreased down to nearly zero within 3000 times of voltage cycles, Pt/SnO_2-based electrocatalysts exhibited considerably longer durability. Sasaki *et al.*[107] prepared electrocatalysts with different oxide supports, Pt/SnO_2, Pt/Nb–SnO_2, Pt/Sb–SnO_2, and Pt/Al–SnO_2, as well as Pt/TiO_2. It was demonstrated that electrocatalysts using alternative catalyst support materials exhibit comparable electrochemical performance to the conventional Pt/C electrocatalysts. Especially, the use of carbon-free oxide-supported electrocatalysts can be an ultimate solution to prevent the carbon corrosion problem. Kakinuma *et al.*[108] synthesized a Pt catalyst supported on $Sn_{0.96}Sb_{0.04}O_{2-\delta}$ with a random network structure for the cathode of the polymer electrolyte fuel cell (PEFC). The $Sn_{0.96}Sb_{0.04}O_{2-\delta}$ support, synthesized by the flame combustion method, was in the form of nanometer-sized particles with a partially agglomerated structure similar to that of carbon black (CB) and with a high surface area, 125 $m^2\ g^{-1}$. The ECA was 50.2 $m^2\ g^{-1}$ (Pt) initially, and the values were maintained at a high value during the potential step cycle test (0.9–1.3 V). The oxygen reduction activity of the Pt/$Sn_{0.96}Sb_{0.04}O_{2-\delta}$ catalyst exceeded that of Pt on carbon black. Fan *et al.*[109] prepared hierarchical structure SnO_2 with two-dimensional (2D) nanosheets building blocks as support material for Pt nanoparticles (NPs). The superior catalytic performance may arise from the unique multiscale structure and morphology of the SnO_2 support, which process extraordinary promotional effect on Pt catalyst. Dou *et al.*[110] synthesized tin oxide nanocluster (SnO_2) with parallel nanorods *via* a hard template method and explored as the anode catalyst support for proton exchange membrane fuel cells (PEMFCs). Electrochemical measurements showed that Pt/SnO_2 exhibited significantly enhanced electrochemical stability than Pt/C under high potential electrooxidation and potential cycling. The Pt/SnO_2 catalyst reserved most of its electrochemically active surface area (ECA) under 10 h potential hold at 1.6 V while its ECA degradation rate was one order of magnitude lower than Pt/C under potential cycling between 0.6 and 1.2 V. Elezovic *et al.*[111,112] t synthesized two different tin oxide based supports, Sb–SnO_2 and Ru–SnO_2, by hydrazine reduction method. Pt catalysts on Sb and Ru doped SnO_2 support exhibited catalytic activities comparable to Pt on commercial carbon based support. Stability tests were also performed. Determined small loss of electrochemical active surface area of the Pt catalyst on Sb doped tin oxide support, after repetitive cycling, indicated high stability and durability of this cathode for prospective fuel cells application. Hoque *et al.*[113] made unique tin oxide-mesoporous carbon (SnO_2–CMK-3) composites have been synthesized as platinum nanoparticle electrocatalyst supports for low temperature fuel cell applications. The improvements to the oxygen reduction reaction (ORR) kinetics were observed, with Pt/SnO_2–CMK-3 providing a kinetic current density of 3.40 mA cm^{-2} at an electrode potential of 0.9 V *vs.* RHE. The improved performance of Pt/SnO_2–CMK-3 for EOR and ORR was attributed to the beneficial impact of the support properties, along with potential interactions occurring between the support and catalyst particles. Zhang *et al.*[114] referred a novel nanostructural Pt/SnO_2/C catalyst synthesized by depositing Pt nanoparticles on the SnO_2/C surface. Electrochemical measurements showed that specific activity towards oxygen reduction reaction (ORR) of Pt/SnO_2/C catalysts was 2.3 times as high as that of conventional Pt/C catalysts. Accelerated degradation test (ADT) indicated that electrochemical stability of Pt/SnO_2/C was twice as high as that of conventional Pt/C catalysts. The improved performance can be attributed to the presence of Pt/SnO_2/C triple junction nanostructures, in which Pt nanoparticles were thermodynamically favored to deposit at the SnO_2/C junctions, and then be anchored simultaneously by both SnO_2 and C. Tsukatsune *et al.*[115] showed that using tin oxide (SnO_2) and niobium-doped tin oxide (Nb–SnO_2) as alternative electrocatalyst support materials can effectively solve the issue of carbon corrosion in polymer electrolyte fuel cell (PEFC) cathodes. The dependence of ECSA and ORR activity on Pt particle size, support surface area, Pt loading and residual Cl^- ion contamination was examined. The ECSA of Pt/SnO_2 and Pt/Nb–SnO_2 electrocatalysts was comparable to Pt/Vulcan after optimization of the normalized support surface area. However, in this study, since the specific surface area of supports was not large enough, an increase in ECSA derived by decreasing Pt particles size resulted in a decrease in specific activity. Nb-doping of the SnO_2 support also increased the specific activity, due to improved electronic conductivity. Consequently, oxide-supported PEFC electrocatalysts with high ORR activity require oxide supports with; (i) large specific surface area, (ii) high electronic conductivity, and (iii) negligible impurities. Dou *et al.*[116] prepared Sb-doped SnO_2 (ATO) nanoparticles and used as highly stable catalyst support for proton exchange membrane fuel cells. The obtained results demonstrated significantly improved durability if compared to Pt/C. After 800 cycles between 0.6 and 1.2 V *vs.* NHE, the ORR mass activity of Pt/ATO dropped by 35.1%, which was much lower than that of Pt/C (78.4%). The enhanced electrochemical stability of Pt/ATO is attributed to the high stability of ATO support and the strong interaction between Pt and ATO.

4. Conclusion

Generally, the electrocatalytic activity of supported Pt and Pt–M alloy catalysts is referred as mass activity (MA) or specific activity (SA), *i.e.* it is normalized with respect to the mass (MA) or the surface area (SA) of the catalyst in the electrode. Regarding the catalysts supported on metal oxide materials, their mass activity was generally lower than that of the same catalysts supported on carbon, due to the lower surface area of the oxide substrates.[117] Thus, to increase the mass activity of supported catalysts, research goals have to be addressed to the achievement of support with high surface area. Having in mind all above stated results, it could be concluded that some problems referred earlier,[117] were resolved. Namely, the high surface area, one of the most important demands was achieved.[81,108,111,116] Therefore, tin oxide and titanium oxide based supports were synthesized with sufficiently high surface area.

High stability of these materials under accelerated stability tests is also achieved.[85,105,106,114,115] The main remark related to prospective commercial application is that there is still small number of investigations and testing the Pt catalysts on metal oxide supports in membrane electrode assembly form. The most of the literature results on this topic is performed as single electrode (single electrochemical reaction) testing. The other important issue is related to proper determination of the catalytic activities for oxygen reduction, as the whole performance of fuel cell is much more influenced by its slow kinetics and high overpotential. To ensure that results are comparable to other literature values one should pay attention on the following: (a) the proper rotating disc electrode measurements – the optimal catalyst loading applied; (b) proper correction for IR drop ohmic resistance, especially in low concentration electrolytes, such as commonly used 0.1 mol dm^{-3} $HClO_4$; (c) proper formation of the thin film catalyst from the ink, to ensure reproducibility.

Acknowledgements

This work was financially supported by Ministry of Education, Science and Technological Development, Republic of Serbia, under contract number 172054. Electron microscopy characterization was performed at the National Center for Electron Microscopy, Lawrence Berkeley National Laboratory, which is supported by the Office of Science, Office of Basic Energy Sciences, of the U.S. Department of Energy under Contract no. DE-AC02-05CH11231.

References

1 A. Morozan, B. Jousselme and S. Palacin, *Energy Environ. Sci.*, 2011, **4**, 1238–1254.
2 U. A. Paulus, T. J. Schmidt, H. A. Gaisteiger and R. J. Behm, *J. Electroanal. Chem.*, 2001, **495**, 134–145.
3 F. Maillard, M. Martin, F. Gloaguen and J. M. Leger, *Electrochim. Acta*, 2002, **47**, 3431–3440.
4 R. Benitez, A. M. Chaparro and L. Daza, *J. Power Sources*, 2005, **151**, 2–10.
5 Q. Huang, H. Yang, Y. Tang, T. Lu and D. L. Akins, *Electrochem. Commun.*, 2006, **8**, 1220–1224.
6 Z. Liu, Z. Q. Tian and S. P. Jiang, *Electrochim. Acta*, 2006, **52**, 1213–1220.
7 H. A. Gasteiger, J. E. Panels and S. G. Yan, *J. Power Sources*, 2004, **127**, 162–171.
8 T. Toda, H. Igarashi, H. Uchida and M. Watanabe, *J. Electrochem. Soc.*, 1999, **146**, 3750–3756.
9 C. A. Reiser, L. Bregoli, T. W. Patterson, S. Y. Jung, J. D. Yang, M. L. Perry and T. D. Jarvi, *Electrochem. Solid-State Lett.*, 2005, **8**, A273–A276.
10 A. Pozio, R. F. Silva, M. de Francesco, F. Cardellini and L. Giorgi, *Electrochim. Acta*, 2002, **48**, 255–262.
11 P. Ma, T. Haolin, M. Shichun and Y. Runzhang, *J. Mater. Res.*, 2004, **19**, 2279–2284.
12 G. Girishkumar, K. Vinodgopal and P. V. Kamat, *J. Phys. Chem. B*, 2004, **108**, 19960–19966.
13 Z. Q. Tian, S. P. Jiang, Y. M. Liang and P. K. Shen, *J. Phys. Chem. B*, 2006, **110**, 5343–5350.
14 Z. Liu, X. Lin, J. Y. Lee, W. Zhang, M. Han and L. M. Gan, *Langmuir*, 2002, **18**, 4054–4060.
15 K. Vinodgopal, M. Haria, D. Meisel and P. Kamat, *Nano Lett.*, 2004, **4**, 415–418.
16 J. Perez, E. R. Gonzalez and E. A. Ticianelli, *Electrochim. Acta*, 1998, **44**, 1329–1339.
17 G. Tamizhmani, J. P. Dodelet and D. Guay, *J. Electrochem. Soc.*, 1996, **143**, 18–23.
18 N. M. Markovic, H. Gasteiger and P. N. Ross, *J. Electrochem. Soc.*, 1997, **144**, 1591–1597.
19 L. Genies, R. Faure and R. Durand, *Electrochim. Acta*, 1998, **44**, 1317–1327.
20 U. A. Paulus, T. J. Schmidt, H. A. Gasteiger and R. J. Behm, *J. Electroanal. Chem.*, 2001, **495**, 134–145.
21 A. Ayad, Y. Naimi, J. Bouet and J. F. Fauvarque, *J. Power Sources*, 2004, **130**, 50–55.
22 S. K. Zecevic, J. S. Wainright, M. H. Litt, S. Y. Gojkovic and R. F. Savinell, *J. Electrochem. Soc.*, 1997, **144**, 2973–2982.
23 Z. Liu, Z. Q. Tian and S. P. Jiang, *Electrochim. Acta*, 2006, **52**, 1213–1220.
24 O. J. Curnick, B. G. Pollet and P. M. Mendes, *RSC Adv.*, 2012, **2**, 8368–8374.
25 K. J. J. Mayrhofer, D. Strmcnik, B. B. Blizanac, V. Stamenkovic, M. Arenz and N. M. Markovic, *Electrochim. Acta*, 2008, **53**, 3181–3188.
26 K. Yoshii, T. Tsuda, T. Arimura, A. Imanishi, T. Torimotoe and S. Kuwabata, *RSC Adv.*, 2012, **2**, 8262–8264.
27 J. Speder, L. Altmann, M. Baumer, J. J. K. Kirkensgaard, K. Mortensenc and M. Arenz, *RSC Adv.*, 2014, **4**, 14971–14978.
28 B. Singh and E. Dempsey, *RSC Adv.*, 2013, **3**, 2279–2287.
29 M. Sahoo, B. P. Vinayan and S. Ramaprabhu, *RSC Adv.*, 2014, **4**, 26140–26148.
30 W. Yuan, S. Lu, Y. Xiang and S. P. Jiang, *RSC Adv.*, 2014, **4**, 46265–46284.
31 S. Y. Wang, S. P. Jiang, T. J. White, J. Guo and X. Wang, *J. Phys. Chem. C*, 2009, **113**, 18935–18945.
32 J. G. Zhou, X. T. Zhou, X. H. Sun, R. Y. Li, M. Murphy, Z. F. Ding, X. L. Sun and T. K. Sham, *Chem. Phys. Lett.*, 2007, **437**, 229–232.
33 Y. Tian, Y. Liu, J. X. Zhao and Y. Ding, *RSC Adv.*, 2015, **5**, 34070–34077.
34 A. Godinez-Garcia and D. F. Gervasio, *RSC Adv.*, 2014, **4**, 42009–42013.
35 R. Jager, E. Hark, P. E. Kasatkin and E. Lust, *J. Electrochem. Soc.*, 2014, **161**, F861–F867.
36 T. Nagai, H. Murata and Y. Morimoto, *J. Electrochem. Soc.*, 2014, **161**, F789–F794.
37 Z. Wang, E. Tada and A. Nishikata, *J. Electrochem. Soc.*, 2014, **161**, F380–F385.
38 S. R. Dhanushkodi, M. Schwager, D. Todd and W. Merida, *J. Electrochem. Soc.*, 2014, **161**, F1315–F1322.
39 Y. Li, K. Moriyama, W. Gu, S. Arisetty and C. Y. Wang, *J. Electrochem. Soc.*, 2015, **162**, F834–F842.

40 T. S. Olson, A. A. Dameron, K. Wood, S. Pylpenko, K. E. Hurst, S. Christensen, J. B. Bult, D. S. Ginley, R. O'Hayre, H. Dinh and T. Gennett, *J. Electrochem. Soc.*, 2013, **160**, F389–F394.
41 Z. Zhang, J. Liu, J. Gu, J. Su and L. Cheng, *Energy Environ. Sci.*, 2014, **7**, 2535–2558.
42 L. Chen, A. C. Cooper, G. P. Pez and H. Cheng, *J. Phys. Chem. C*, 2008, **112**, 1755–1758.
43 N. R. Elezovic, B. M. Babic, V. R. Radmilovic, L. M. Vracar and N. V. Krstajic, *Electrochim. Acta*, 2009, **54**, 2404–2409.
44 N. R. Elezović, B. M. Babić, V. R. Radmilović, S. Gojković, N. V. Krstajić and L. M. Vračar, *J. Power Sources*, 2008, **175**, 250–255.
45 Y. Wang, E. R. Fachini, G. Cruz, Y. Zhu, Y. Ishikawa, J. A. Colucci and C. R. Cabrera, *J. Electrochem. Soc.*, 2001, **148**, C222–C226.
46 P. Justin and G. Ranga Rao, *Int. J. Hydrogen Energy*, 2011, **36**, 5875–5884.
47 D. C. Papageorgopoulos, M. Keijzer and F. A. de Bruijn, *Electrochim. Acta*, 2012, **48**, 197–204.
48 T. Ioroi, T. Akita, S. Yamazaki, Z. Siroma, N. Fujiwara and K. Yasuda, *Electrochim. Acta*, 2006, **52**, 491–498.
49 T. Ioroi, N. Fujiwara, Z. Siroma, K. Yasuda and Y. Miyazaki, *Electrochem. Commun.*, 2002, **4**, 442–446.
50 Z. Yan, J. Xie, J. Jing, M. Zhang, W. Wei and S. Yin, *Int. J. Hydrogen Energy*, 2002, **37**, 15948–15955.
51 B. S. Hobbs and A. C. C. Tseung, *J. Electrochem. Soc.*, 1975, **122**, 1174–1177.
52 M. A. Butler, *J. Appl. Phys.*, 1977, **48**, 1914–1920.
53 M. Pourbaix, *Atlas of Electrochemical Equilibria in Aqueous Solutions*, Pergamon, London, 1966, p. 280.
54 D. V. Esposito and J. G. Chen, *Energy Environ. Sci.*, 2011, **4**, 3900–3912.
55 M. C. Weidman, D. V. Esposito, I. J. Hsu and J. G. Chen, *J. Electrochem. Soc.*, 2010, **57**, F179–F188.
56 E. Antolini and E. R. Gonzalez, *Appl. Catal., B*, 2010, **96**, 245–266.
57 E. C. Weigert, S. Arisetty, S. G. Advani, A. K. Prasad and J. G. Chen, *J. New Mater. Electrochem. Syst.*, 2008, **11**, 243–251.
58 Y. Wang, S. Song, V. Maragou, P. K. Shen and P. Tsiakaras, *Appl. Catal., B*, 2009, **89**, 223–228.
59 Y. Hara, N. Minami, H. Matsumoto and H. Itagaki, *Appl. Catal., A*, 2007, **332**, 289–296.
60 Q. Zhu, S. Zhou, X. Wang and S. Dai, *J. Power Sources*, 2009, **193**, 495–500.
61 H. Chhina, S. Campbell and O. Kesler, *J. Power Sources*, 2007, **164**, 431–440.
62 Z. Shengsheng, Z. Hong, Y. Hongmei, H. Junbo, Y. Baolian and M. Pingwen, *Chin. J. Catal.*, 2007, **28**, 109–111.
63 Z. J. Mellinger, E. C. Weigert, A. L. Stottlemyer and J. G. Chen, *Electrochem. Solid-State Lett.*, 2008, **11**, B63–B67.
64 E. C. Weigert, D. V. Esposito and J. G. Chen, *J. Power Sources*, 2009, **193**, 501–506.
65 P. K. Shen, S. Yin, Z. Li and C. Chen, *Electrochim. Acta*, 2010, **55**, 7969–7974.
66 D. V. Esposito and J. G. Chen, *Energy Environ. Sci.*, 2011, **4**, 3900–3912.
67 R. Ganesan, D. J. Ham and J. Lee, *Electrochem. Commun.*, 2007, **9**, 2576–2579.
68 R. Xu, F. Xu, M. Pan and S. Mu, *RSC Adv.*, 2013, **3**, 764–773.
69 N. R. Elezovic, B. M. Babic, P. Ercius, V. R. Radmilovic, L. M. Vracar and N. V. Krstajic, *Appl. Catal., B*, 2012, **124**, 390–397.
70 N. R. Elezovic, B. M. Babic, L. Gajić-Krstajic, P. Ercius, V. R. Radmilovic, N. V. Krstajic and L. M. Vračar, *Electrochim. Acta*, 2012, **69**, 239–246.
71 M. D. Obradović, S. L. Gojković, N. R. Elezović, P. Ercius, V. R. Radmilović, L. M. Vračar and N. V. Krstajić, *J. Electroanal. Chem.*, 2012, **671**, 24–32.
72 A. C. Garcia and E. A. Ticianelli, *Electrochim. Acta*, 2013, **106**, 453–459.
73 Z. Yan, W. Wei, J. Xie, S. Meng, X. Lü and J. Zhu, *J. Power Sources*, 2013, **222**, 218–224.
74 F. Li, H. Gong, Y. Wang, H. Zhang, Y. Wang, S. Liu, S. Wang and C. Sun, *J. Mater. Chem. A*, 2014, **2**, 20154–20163.
75 L. Xiong, L. Zheng, C. Liu, L. Jin, Q. Liu and J. Xu, *J. Electrochem. Soc.*, 2015, **162**, F468–F473.
76 G. R. Dieckmann and S. H. Langer, *Electrochim. Acta*, 1998, **44**, 437–444.
77 L. M. Vracar, S. L. Gojkovic, N. R. Elezovic, V. R. Radmilovic, M. M. Jaksic and N. V. Krstajic, *J. New Mater. Electrochem. Syst.*, 2006, **9**, 99–106.
78 E. Slavcheva, V. Nikolova, T. Petkova, E. Lefterova, I. Dragieva, T. Vitanov and E. Budevski, *Electrochim. Acta*, 2005, **50**, 5444–5448.
79 K. Sasaki, L. Zhang and R. R. Adzic, *Phys. Chem. Chem. Phys.*, 2008, **10**, 159–167.
80 K. W. Park and K. S. Seul, *Electrochem. Commun.*, 2007, **9**, 2256–2260.
81 N. R. Elezovic, B. M. Babic, L. Gajic-Krstajic, V. Radmilovic, N. V. Krstajic and L. Vracar, *J. Power Sources*, 2010, **195**, 3961–3968.
82 N. R. Elezovic, B. M. Babic, V. R. Radmilovic, L. M. Vracar and N. V. Krstajic, *Electrochim. Acta*, 2011, **56**, 9020–9026.
83 B. Y. Xia, S. Ding, H. B. Wu, X. Wang and X. Wen (David), *RSC Adv.*, 2012, **2**, 792–796.
84 F. Shi, L. R. Baker, A. Hervier, G. A. Somorjai and K. Komvopoulos, *Nano Lett.*, 2013, **13**, 4469–4474.
85 A. Kumar and V. Ramani, *J. Electrochem. Soc.*, 2013, **160**, F1207–F1215.
86 S. Siracusano, A. Stassi, E. Modica, V. Baglio and A. S. Arico, *Int. J. Hydrogen Energy*, 2013, **38**, 11600–11608.
87 C. Zhang, H. Yu, Y. Li, L. Fu, Y. Gao, W. Song, Z. Shao and B. Yi, *J. Electroanal. Chem.*, 2013, **701**, 14–19.
88 K. Tiido, N. Alexeyeva, M. Couillard, C. Bock, B. R. MacDougall and K. Tammeveski, *Electrochim. Acta*, 2013, **107**, 509–517.
89 D. Huang, B. Zhang, J. Bai, Y. Zhang, G. Wittstock, M. Wang and Y. Shen, *Electrochim. Acta*, 2014, **130**, 97–103.
90 S. Meenakshi, K. G. Nishanth, P. Sridhar and S. Pitchumani, *Electrochim. Acta*, 2014, **135**, 52–59.

91 I. Savych, J. Bernard d'Arbigny, S. Subianto, S. Cavaliere, D. J. Jones and J. Rozière, *J. Power Sources*, 2014, **257**, 147–155.
92 W. A. Rigdon and X. Huang, *J. Power Sources*, 2014, **272**, 845–859.
93 B. Ruiz-Camacho, O. Martínez-Álvarez, H. H. Rodríguez-Santoyo and V. Granados-Alejo, *J. Electroanal. Chem.*, 2014, **725**, 19–24.
94 K. Jukk, N. Kongi, A. Tarre, A. Rosental, A. B. Treshchalov, J. Kozlova, P. Ritslaid, L. Matisen, V. Sammelselg and K. Tammeveski, *J. Electroanal. Chem.*, 2014, **735**, 68–76.
95 C. W. Liu, C. M. Lai, J. N. Lin, L. D. Tsai and K. W. Wang, *RSC Adv.*, 2014, **4**, 15820–15824.
96 Y. Li, C. Liu, Y. Liu, B. Feng, L. Li, H. Pan, W. Kellogg, D. Higgins and G. Wu, *J. Power Sources*, 2015, **286**, 354–361.
97 C. Odetola, L. Trevani and E. Bradley Easton, *J. Power Sources*, 2015, **294**, 254–263.
98 X. L. Sui, Z. B. Wang, Y. F. Xia, M. Yang, L. Zhao and D. M. Gu, *RSC Adv.*, 2015, **5**, 35518–35523.
99 H. Shintani, Y. Kojima, K. Kakinuma, M. Watanabe and M. Uchida, *J. Power Sources*, 2015, **294**, 292–298.
100 N. R. Elezović, B. M. Babić, V. R. Radmilovic, L. M. Vračar and N. V. Krstajić, *Appl. Catal., B*, 2013, **140–141**, 206–212.
101 N. R. Elezovic, P. Ercius, J. Kovac, V. R. Radmilovic, B. M. Babic and N. V. Krstajic, *J. Electroanal. Chem.*, 2015, **739**, 164–171.
102 A. L. Santos, D. Profeti and P. Olivi, *Electrochim. Acta*, 2005, **50**, 2615–2621.
103 M. S. Saha, R. Li, M. Cai and X. Sun, *Electrochem. Solid-State Lett.*, 2007, **10**, B130–B133.
104 K. S. Lee, I. S. Park, Y. H. Cho, D. S. Jung, N. Jung, H. Y. Park and Y. E. Sung, *J. Catal.*, 2008, **258**, 143–152.
105 F. Takasaki, S. Matsuie, Y. Takabatake, Z. Noda, A. Hayashi, Y. Shiratori, K. Ito and K. Sasaki, *J. Electrochem. Soc.*, 2011, **158**, B1270–B1275.
106 F. Takasaki, Z. Noda, A. Masao, Y. Shiratori, K. Ito and K. Sasaki, *ECS Trans.*, 2009, **25**, 831–837.
107 K. Sasaki, F. Takasaki, Z. Noda, S. Hayashi, Y. Shiratori and K. Ito, *ECS Trans.*, 2010, **33**, 473–482.
108 K. Kakinuma, M. Uchida, T. Kamino, H. Uchida and M. Watanabe, *Electrochim. Acta*, 2011, **56**, 2881–2887.
109 Y. Fan, J. Liu, H. Lu, P. Huang and D. Xu, *Electrochim. Acta*, 2012, **76**, 475–479.
110 M. Dou, M. Hou, D. Liang, W. Lu, Z. Shao and B. Yi, *Electrochim. Acta*, 2013, **92**, 468–473.
111 N. R. Elezović, B. M. Babić, V. R. Radmilovic and N. V. Krstajić, *J. Electrochem. Soc.*, 2013, **160**, F1151–F1158.
112 N. R. Elezovic, V. R. Radmilovic, J. Kovac, B. M. Babic, L. M. Gajic-Krstajic and N. V. Krstajic, *RSC Adv.*, 2015, **5**, 15923–15929.
113 M. A. Hoque, D. C. Higgins, F. M. Hassan, J. Y. Choi, M. D. Pritzker and Z. Chen, *Electrochim. Acta*, 2014, **121**, 421–427.
114 N. Zhana, S. Zhang, C. Du, Z. Wang, Y. Shao, F. Kong, Y. Lin and G. Yin, *Electrochim. Acta*, 2014, **117**, 413–419.
115 T. Tsukatsune, Y. Takabatake, Z. Noda, T. Daio, A. Zaitsu, S. M. Lyth, A. Hayashi and K. Sasaki, *J. Electrochem. Soc.*, 2014, **161**, F1208–F1213.
116 M. Dou, M. Hou, F. Wang, D. Liang, Q. Zhao, Z. Shao and B. Yi, *J. Electrochem. Soc.*, 2014, **161**, F1231–F1236.
117 E. Antolini and E. R. Gonzalez, *Solid State Ionics*, 2009, **180**, 746–763.